Supporting Information

Modulating spin dynamics of cyclic Ln^{III}–radical complexes (Ln^{III} = Tb, Dy) by using phenyltrifluoroacetylacetonate coligand

Xue-Lan Mei, Rui-Na Liu, Chao Wang, Pei-Pei Yang, Li-Cun Li*, Dai-Zheng Liao

Department of Chemistry and Key Laboratory of Advanced Energy Materials Chemistry, Nankai University, Tianjin 300071, PR China

Table S1. Selected bond lengths (Å) and bond angles (deg) for complexes **1**-**3**.

	Complex **1**	Complex **2**	Complex **3**	$[Tb(hfac)_2(NITpPy)]_2$	
Ln1-O1(Phtfac)	2.340(3)	2.329(4)	2.316(5)	Tb1-O3(hfac)	2.365(4)
Ln1-O2(Phtfac)	2.359(3)	2.346(4)	2.327(5)	Tb1-O4(hfac)	2.345(4)
Ln1-O3(Phtfac)	2.347(4)	2.336(4)	2.332(5)	Tb1-O7(hfac)	2.329(4)
Ln1-O4(Phtfac)	2.374(3)	2.364(4)	2.356(4)	Tb1-O8(hfac)	2.361(4)
Ln1-O5(Phtfac)	2.346(3)	2.318(4)	2.314(5)	Tb1-O6(hfac)	2.344(4)
Ln1-O6(Phtfac)	2.340(3)	2.328(4)	2.320(4)	Tb1-O5(hfac)	2.350(4)
Ln1-O7(Rad)	2.431(3)	2.426(4)	2.406(4)	Tb1-O1(Rad)	2.364(4)
Ln1-N3	2.619(4)	2.609(5)	2.596(5)	Tb1-N1	2.593(4)
N1-O7	1.281(5)	1.288(6)	1.284(7)	N2-O1	1.291(6)
N2-O8	1.276(5)	1.286(6)	1.273(7)	N3-O2	1.262(6)
O7-Ln1-N3	101.72(12)	102.05(14)	102. 34(16)	O1-Tb1-N1	104.34(13)
N1-O7-Ln1	138.7(3)	139.2 (3)	139.6(4)	N2-O1-Tb1	138.5(3)
N1-C37-N2	109.1(4)	107.8(5)	108.4(6)	N3-C6-N2	108.9(4)
O1-Ln1-N3	76.02(12)	76.10(14)	76.04(18)	O3-Tb1-N1	80.61(13)
O2-Ln1-N3	143.28(12)	143.36(14)	143.74(17)	O4-Tb1-N1	143.44(14)
O3-Ln1-N3	81.60(12)	81.54(15)	81.38(18)	O7-Tb1-N1	81.25(14)
O4-Ln1-N3	76.93(12)	76.61(14)	76.69(17)	O8-Tb1-N1	72.45(14)
O5-Ln1-N3	69.75(11)	69.78(14)	69.67(17)	O6-Tb1-N1	71.45(13)
O6-Ln1-N3	141.50(12)	141.64(14)	141.68(19)	O5-Tb1-N1	141.33(14)
The shortest Ln...Ln distance between the dimer units	9.389	9.397	9.439	The shortest Ln...Ln distance between the dimer units	10.714

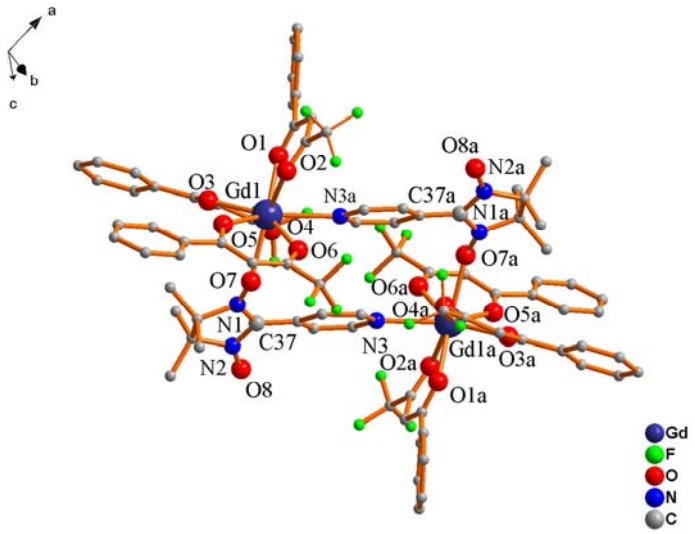

Fig. S1. The molecular structure of **1**. H atoms are not shown for the sake of clarity.

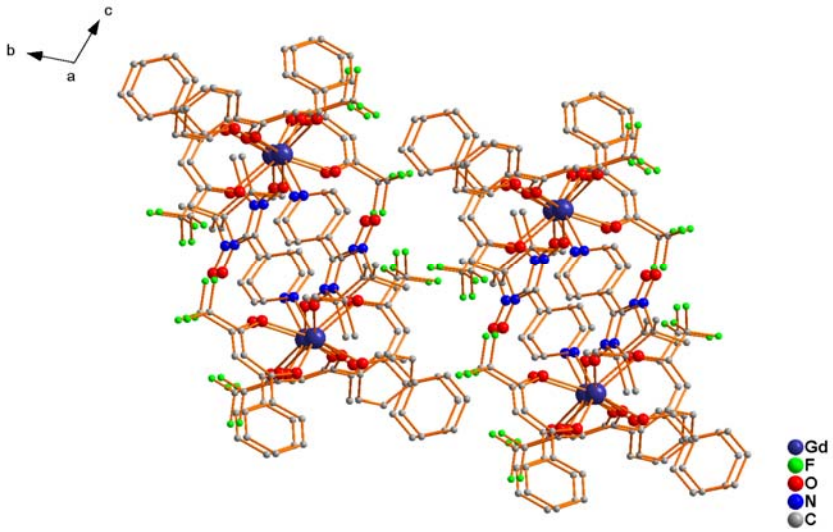

Fig. S2. Packing diagram of complex **1**. H atoms are not shown for the sake of clarity.

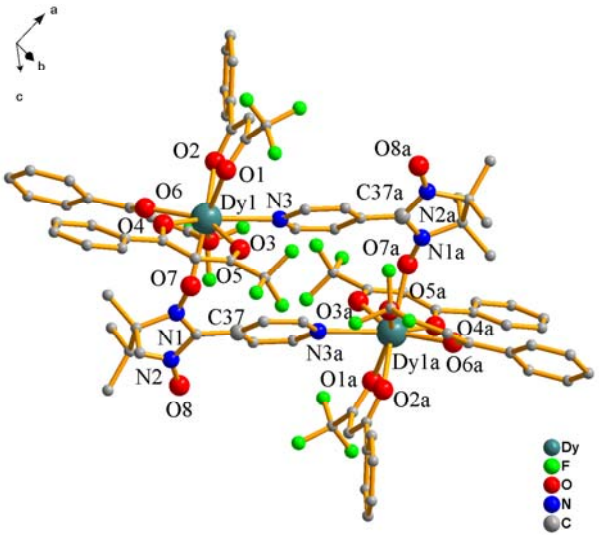

Fig. S3. The molecular structure of **3**. H atoms are not shown for the sake of clarity.

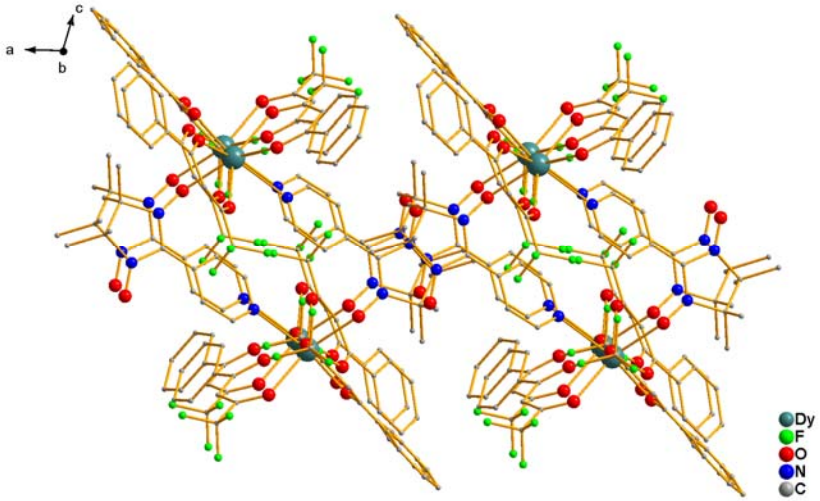

Fig. S4. Packing diagram of complex **3**. H atoms are not shown for the sake of clarity.

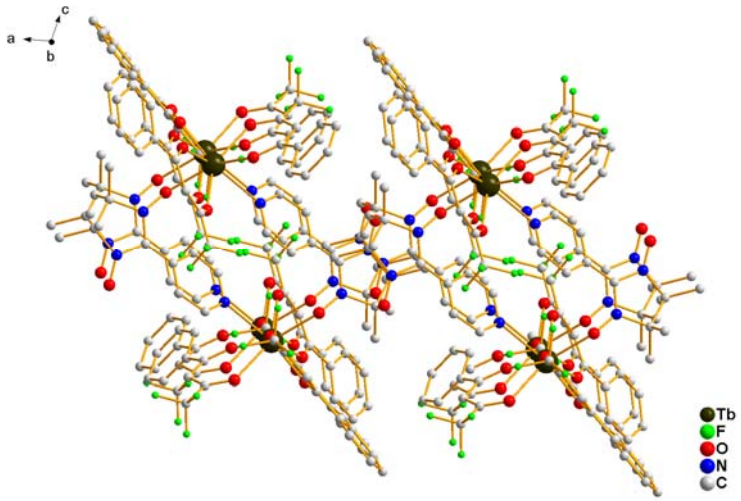

Fig. S5. Packing diagram of complex **2**. H atoms are not shown for the sake of clarity.

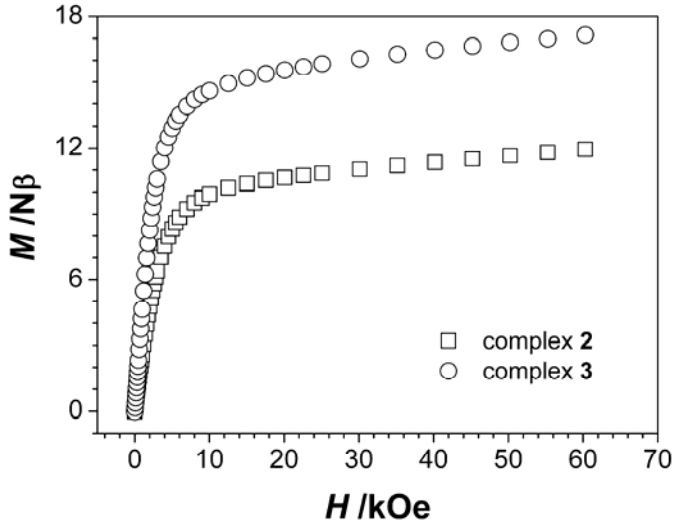

Fig. S6. *M* versus *H* plots for **2** and **3** at 2.0 K.

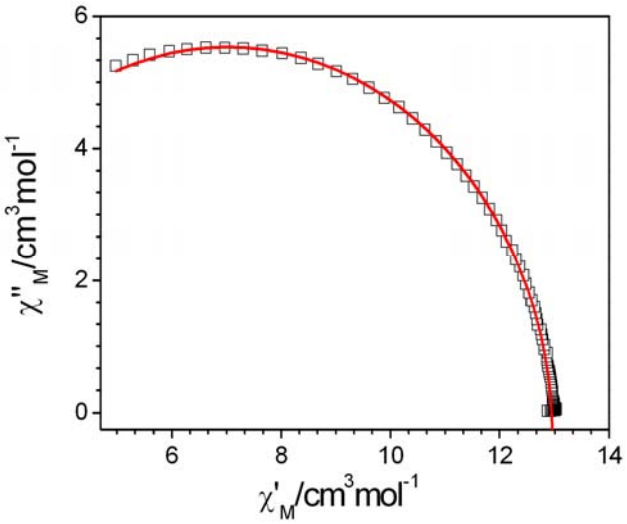

Fig. S7. The Cole–Cole plot at 3 K of **2** in zero-dc field. The red solid line represents the best fitting results obtained with a Debye model.

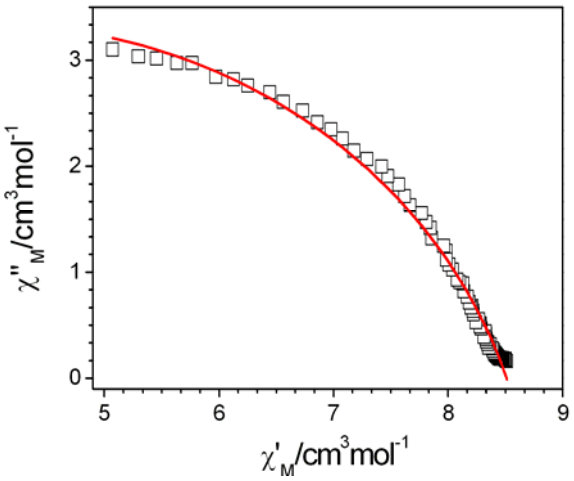

Fig. S8. The Cole–Cole plot at 5 K of **3** in 3 kOe dc field. The red solid line represents the best fitting results obtained with a Debye model.

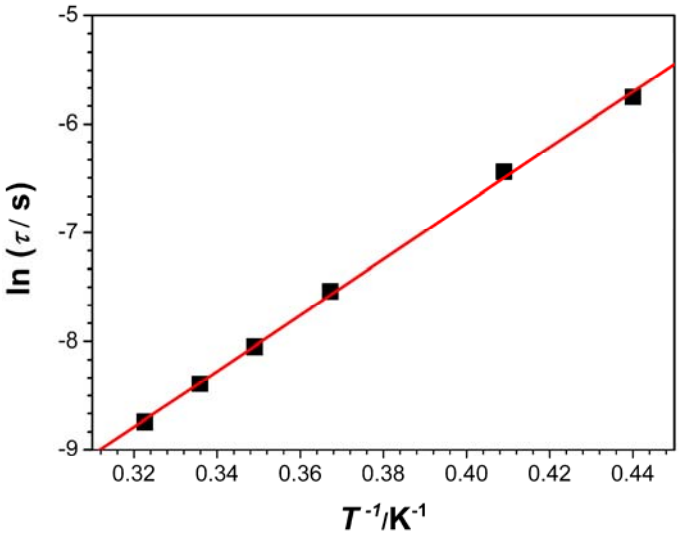

Fig. S9. lnτ *vs.* 1/T plot for **2**. The solid line represents the least-squares fit of the experimental data to Arrhenius law.

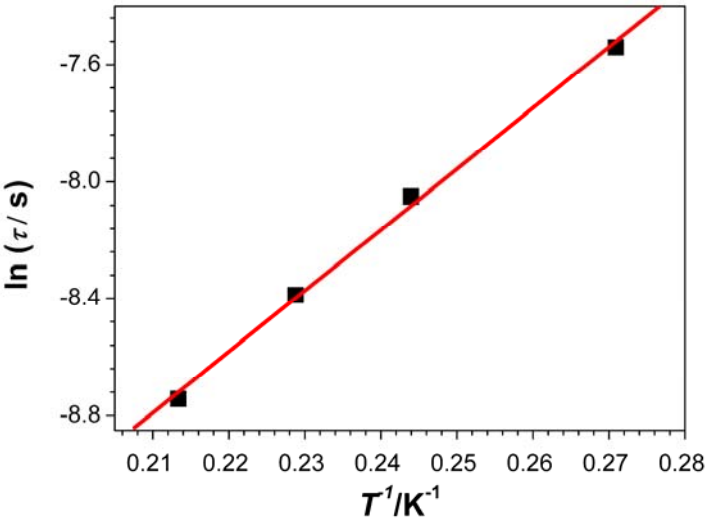

Fig. S10. lnτ *vs.* 1/T plot for **3**. The solid line represents the least-squares fit of the experimental data to Arrhenius law.